



NIRSpec Performance Report NPR-2014-003

Author(s): G. Giardino
Date of Issue: September 25, 2014
Version: 1.0

European Space Research
and Technology Centre
Keplerlaan 1
2201 AZ Noordwijk
The Netherlands
Tel. (31) 71 5656565
Fax (31) 71 5656040
www.esa.int

The wavelength stability of the CAA sources across two test cycles of NIRSpec FM2

Abstract:

The NIRSpec calibration assembly (CAA) houses eleven sources to be used for the instrument calibration and monitoring. In this document, we analyse the wavelength stability of the absorption lines of the REF source and of the emission features of the LINE1/2/3 sources of the CAA, across the two thermal cycles that NIRSpec underwent for Calibration and Performance Verification. To perform this analysis, an accurate parametric model of NIRSpec optical properties had to be derived for each of the two test cycles. We conclude that the lines of the REF source are stable in wavelength within 0.01 nm while those of the LINE sources are stable within 0.02-0.04 nm.

1 INTRODUCTION AND METHODOLOGY

The purpose of the NIRSpec calibration assembly (CAA) is to enable on-orbit calibration and monitoring of a number of important instrument parameters such as (i) the geometric distortion between the Micro Shutter Array and the focal plane, (ii) the instrument throughput as a function of both field angle and wavelength, and (iii) the dispersion of the various spectral elements. It is therefore important to understand the behavior of the CAA lamps throughout the NIRSpec lifetime.

The stability of the CAA sources fluxes during one thermal cycle was demonstrated by Boeker & Giardino (2011). In this report, we analyze the wavelength stability of the CAA spectral reference sources across two cryo-vacuum test cycles. The wavelength stability of the lines of the CAA sources is also a necessary pre-requisite if one wants to use the CAA to optimize the NIRSpec parametric model, which is used for the instrument wavelength calibration, in the absence of an external wavelength reference source, such as the Argon lamp.

NIRSpec Flight Model 2 (FM2) underwent two cryo-vacuum test cycles during the Performance Verification and Calibration (PVC) campaign that took place in 2013 at IABG, Ottobrunn, in Germany. Hereafter, we will refer to these two test cycles as Cycle 1 (roughly 40 days of science exposures over January and the beginning of February) and Cycle 2 (about

10 days of science data over the end of July and the beginning of August). For details on the test setup and the on-ground calibration sources mentioned in the following sections, please refer to Birkmann (2011a).

During the campaign, data were taken with all dispersive elements of NIRSpec, with the appropriate internal and external calibration sources. To analyze the wavelength stability of the REF source, data from the test sequences MOS-MODEL (Cycle 1) and MOS-COMBO-42 (Cycle 2) were used. To compare the wavelength stability of the LINE sources across the two test cycles data from the test sequences MOS-COMBO-41 (Cycle 1) and MOS-COMBO-42 (Cycle 2) were used. The unique identifier of the exposures used for this analysis are summarized in Tables 1 and 2.

This analyses was made possible because we were able to derive an accurate parametric model of NIRSpec optical properties for each of the two test cycles, using exposures of the (external) Argon lamp. For an introduction to NIRSpec parametric model see Dorner (2012b) and Giardino (2013). The procedure and accuracy achieved for the parametric model of Cycle 1 is documented in Dorner (2013). The same procedure was followed in deriving the parametric model for Cycle 2 and similar levels of accuracy were achieved (see below). The set of reference files for the two parametric models are named NIRS_FM2_05_fitted_cal2a and NIRS_FM2_05_fitted_cal2b, for Cycle 1 and Cycle 2 respectively. We consider them sufficiently accurate for the 6 gratings, but not yet completely satisfying for the Prism, so our analysis here is limited to the 6 gratings.

For this analysis of the wavelength stability, only the spectra from the two fixed slits A200_1 and A200_2 were used. For reference, we provide, in Table 3, the average and RMS of the residuals between the model predicted line wavelength and its true value, over all the Argon lines used for the parametric model fitting procedures, for the fixed slits, for Cycle 1 and Cycle 2, for each grating. As it can be seen from the table, the levels of accuracy of the two parametric models are similar (although in Cycle 2 we have only about a quarter of the number of reference points of Cycle 1).

Note that model NIRS_FM2_05_fitted_cal2a for Cycle 1 was derived using the MOS-MODEL sequence as reference and, for NIRS_FM2_05_fitted_cal2b (Cycle 2), we used MOS-COMBO-42 as reference data. This implies that, when comparing REF data from these two test sequences, the Grating Wheel tilt angle is 0 by definition. However, LINE data were not acquired during the MOS-MODEL sequence, so in this case, for Cycle 1, we used data from test sequence MOS-COMBO-41, and therefore had to apply the tilt angle correction when extracting the spectra. The tilt-angle correction is automatically applied by our spectral extraction software, NIPS, using the calibrated tilt-angle sensor-reading relation – see e.g. Alves de Oliveira & Giardino (2014).

For this analysis, the count-rate images were derived from the raw exposure data using the pre-processing pipeline (Birkmann 2011b), with default settings. The two fixed slits spectra were extracted using NIPS extraction pipeline (Dorner 2012a), with the appropriate parametric model. The spectra were oversampled in spectral direction to a final resolution of 2.5 times the default NIPS resolution for each grating, which corresponds to the Nyquist sampling of the nominal resolution of each grating at the central wavelength, so: 0.09 nm for G140H,

Table 1: Unique identifiers (NIDs) for the exposures that were used to analyse the wavelength stability of the NIRSpec CAA/REF source. Data from the MOS-MODEL test sequence and the MOS-COMBO-42 sequence were used, respectively for Cycle 1 and Cycle2.

Grating	Cycle 1 NID	Cycle 2 NID
G140H	9424	14442
G235H	9440	14451
G395H	13129	14457
G140M	9474	14465
G235M	9492	14471
G395M	9504	14480

Table 2: NIDs of the exposures that were used to analyse the wavelength stability of NIRSpec CAA/LINE sources

Lamp	Grating	Cycle 1 NID	Cycle 2 NID
LINE1	G140H	11934	14441
LINE2	G235H	11943	14450
LINE3	G395H	11949	14456

Table 3: Residuals between model predicted wavelength of the Argon lines and their true values, for the two parametric models of NIRSpec, for the two test cycles analyzed here. Residuals are in nm.

Grating	FM2 Cycle 1 [nm]	FM2 Cycle 2 [nm]
G140H	-0.007 ± 0.015	-0.013 ± 0.020
G235H	-0.024 ± 0.028	-0.022 ± 0.023
G395H	-0.039 ± 0.040	-0.043 ± 0.042
G140M	-0.006 ± 0.025	-0.028 ± 0.028
G235M	-0.005 ± 0.047	-0.014 ± 0.046
G395M	-0.006 ± 0.080	-0.055 ± 0.102

0.16 nm for G235H, and 0.27 nm for G395H. Only shorted (dead) pixels were masked during the extraction (and not used).

For all the exposures analyzed here, corresponding flat fields using CAA internal flat-field sources were acquired during the same test sequences. During the analysis, trials were made of extracting the slit spectra and flat-fielding the exposure during NIPS processing, and combining it with the two different methods of deriving the 1D-rectified spectrum, the *collapse* method or the *median* method.

The conclusion was that for the REF lamp the most accurate line measurements can be derived by using the *collapse* method (which is the default method of our extraction pipeline) without flat-fielding the exposure. So this is the approach used in this case. The use of the *collapse* method combined with flat-field division, produces spectra plagued by big spikes due to (unflagged) bad pixels, resulting in less accurate comparison of the line wavelength across the two cycles (or between the two slits). Using the *median* method combined with flat-field division results in slightly less accurate wavelength comparison, in the REF case.

On the other hand, for the LINE sources which have broad emission features, flat fielding the exposure is crucial to accurately compare the emission center wavelengths (especially between the two fixed-slits within the same exposure), so in this case the *median* method combined with flat-field division is the approach that gives the most consistent results and that was used.

2 RESULTS

2.1 CAA/REF source

The CAA/REF source uses an Erbium doped filter and a band pass filter to generate a set of narrow absorption lines in the 1.45 to 1.55 μm region, in the center of NIRSpec Band I. Due to the band pass filters, the REF source can also be used in order 2 and 3 without order overlap, to derive reference data for NIRSpec in Band II and Band III. Extracted spectra with the three high resolution gratings of NIRSpec, for the two cycles, are shown in Fig. 1.

Following the approach outlined in NPR-2013-007 (Birkmann 2013), the positions of the REF absorption lines was computed using the center of gravity (CoG) method by Cameron et al. (1982) (see Appendix A of NPR-2013-007 for details of the computation).

The absorption lines are resolved with the high resolution gratings and partly so with the medium resolution gratings. Nine lines were selected for the comparison between Cycle 1 and Cycle 2. Note that these 9 lines do not include lines 4, 5 and 6 of the six lines selected by Birkmann (2013), for the analysis of NIRSpec wavelength calibration. The difference in wavelength of these two lines, between the cycles, appeared to be significantly larger than for the others selected lines. These three lines are significantly shallower than the others (that is they have lower S/N), so the measured line wavelength is more susceptible to the presence of bad pixels and/or lack of a good p-flat.

To assess the wavelength stability of the REF lines, the high-resolution data, which provide well-resolved lines, are the best suited. The difference of the lines center wavelength between the two Cycles for the two fixed slit spectra are given in Table 4 for G140H, Table 5 for G235H

Table 4: Difference between the measured center-wavelength of the CAA/REF absorption lines in Cycle 1 and Cycle 2, for G140H.

Index	Line wavelength (C1) [μm]	Diff. A200_1 [nm]	Diff. A200_2 [nm]
0	1.45799	0.001	0.007
1	1.46562	0.006	0.012
2	1.47882	0.008	0.002
3	1.48660	0.017	0.001
4	1.51441	0.007	0.007
5	1.51581	0.003	0.008
6	1.52680	0.016	0.009
7	1.52826	0.008	0.005
8	1.52971	0.031	0.006

and Table 6 for G395H. The average and RMS value of these differences over the nine lines, from the two fixed-slit spectra, are: 0.009 ± 0.007 nm for G140H, 0.009 ± 0.027 nm for G235H, and 0.015 ± 0.014 nm for G395H.

For comparison, the average and RMS value of the difference in wavelength of the Argon lines between Cycle 1 and Cycle 2 (using the same MOS-MODEL and MOS-COMBO-42 test sequences) are: 0.008 ± 0.010 nm (over 19 lines) for G140H, 0.001 ± 0.010 nm (over 21 lines) for G235H, and 0.015 ± 0.037 nm (over 31 lines) for G395H.

To gauge the uncertainty associated with our wavelength determinations, one can compare the difference in wavelength of the lines in the spectra of A_200_1 and A_200_2, from the same exposure, since in this case the intrinsic line wavelength is the same. In this case, one derives the following average and RMS values (of the differences between the nine lines averaged over the two exposures from the two Cycles): -0.005 ± 0.009 nm, for G140H, -0.011 ± 0.017 nm, for G235H, and -0.005 ± 0.023 nm for G395H¹, which are very similar to the wavelength differences between the two Cycles.

This and the fact that the average and RMS value of the difference of the REF lines across the two calibration Cycles are comparable to those obtained for the un-resolved Argon lines (our reference) indicates that the absorption lines of the CAA/REF source are stable across the two thermal cycles, within about 0.010 nm (i.e. the uncertainties associated with G140H measurements).

For the purpose of assessing the feasibility of using the CAA/REF lines to optimize NIRSpec parametric model, the accuracy in determining the center wavelength of the REF absorption lines with the medium resolution grating was also analysed, also by comparing the wave-

¹We note that the difference in line wavelength between the two slits appear to be slightly lower for Cycle 1 data than for Cycle two data, likely because of the deteriorating quality of NIRSpec current detectors.

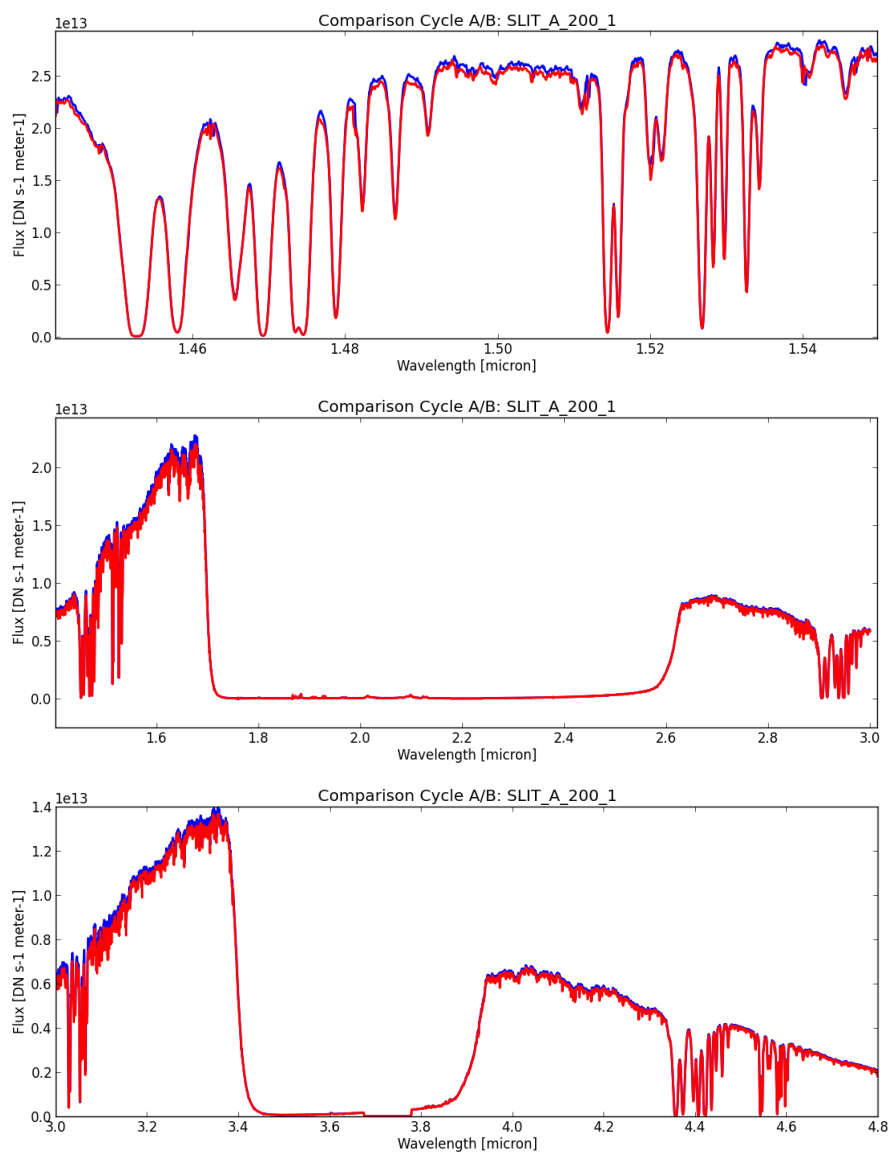


Figure 1: From top to bottom: spectra of the CAA/REF source in order 1 of Grating G140H, order 1 and 2 of Grating G235H and order 2 and 3 of G395H; Cycle 1 data in blue and Cycle 2 data in red. For G235H and G395H the entire wavelength range of the extracted spectra is shown. For G140H we zoomed into the wavelength range where lines are present. Spectra have not been flat fielded.

Table 5: Difference between the measured center-wavelength of CAA/REF lines in Cycle 1 and Cycle 2, for G235H.

Index	Line wavelength (C1) [μm]	Diff. A200_1 [nm]	Diff. A200_2 [nm]
0	2.91601	0.022	0.020
1	2.93130	0.050	0.030
2	2.95770	0.014	0.026
3	2.97326	0.051	0.042
4	1.51439	-0.038	-0.014
5	1.51568	0.005	-0.003
6	1.52675	-0.011	-0.031
7	1.52821	0.002	0.019
8	1.52969	-0.028	-0.002

Table 6: Difference between the measured center-wavelength of CAA/REF lines in Cycle 1 and Cycle 2, for G395H.

Index	Line wavelength (C1) [μm]	Diff. A200_1 [nm]	Diff. A200_2 [nm]
0	4.37397	0.011	0.008
1	4.39684	0.030	0.002
2	4.43647	0.013	0.003
3	4.45977	0.016	0.010
4	4.54324	0.021	0.012
5	4.54744	-0.021	0.033
6	4.58042	0.020	0.016
7	4.58481	0.017	0.012
8	4.58921	0.032	0.039

Table 7: Difference between the measured center-wavelength of CAA/REF lines in Cycle 1 and Cycle 2, for G140M.

Index	Line wavelength (C1) [μm]	Diff. A200_1 [nm]	Diff. A200_2 [nm]
0	1.45274	0.038	-0.025
1	1.45799	-0.009	-0.002
2	1.46571	0.028	0.042
3	1.47418	0.078	0.022
4	1.47888	0.050	0.018
5	1.48649	-0.044	0.076
6	1.51490	-0.017	0.005
7	1.52700	0.036	0.027
8	1.53282	0.058	0.029

length difference between the two cycles. The results are summarised in Table 7 for G140M, Table 8 for G235M, and Table 9 for G395M.

For G140M, the 9 lines selected have acceptable differences (of the order of tenths of nanometers) and the average and RMS value of these differences over the 18 lines from the two spectra are 0.022 ± 0.033 nm. For G235M, there are a number of lines with significantly higher differences (greater than 0.1 nm, in absolute value) than typically seen so far and that would be acceptable to provide an accurate reference for the parametric model optimisation. Excluding these lines, the average and RMS value over the 13 remaining lines in each of the two slits are 0.027 ± 0.028 nm. For G395M, there are even more lines that have a center wavelength difference between the two Cycles greater than 0.1 nm (absolute value) in at least one of the two spectra. Excluding these lines, leaves 9 lines in total (over the two slits) with a sufficiently accurate difference and for these the average and RMS value is -0.007 ± 0.051 nm.

2.2 CAA/LINE sources

The LINE sources provide six broad emission features for each of the gratings distributed over the three different bands. Their extracted, and flat-fielded, spectra are shown in Fig. 2.

Like for the REF source, the position of the individual peaks of the LINE1-3 sources was calculated using the CoG method. The difference between the lines CoGs of source LINE1 in Cycle 1 and Cycle 2, derived using the two fixed slit spectra from G140H, are summarised in Table 10. The average and RMS of this difference over eleven lines in the two slit (line 3 cannot be used in slit A_200_1 because it falls on the detector gap) are 0.015 ± 0.018 nm. Also in this case, the difference in the emission features center wavelengths from the two

Table 8: Difference between the measured center-wavelength of CAA/REF lines in Cycle 1 and Cycle 2, for G235M. Lines where the difference is greater than 0.1 nm in at least one of the two slits are indicated by a dagger symbol.

Index	Line wavelength (C1) [μm]	Diff. A200_1 [nm]	Diff. A200_2 [nm]
0	2.90548	0.059	0.018
1	2.91605	0.028	0.042
2†	2.93144	0.141	-0.026
3	2.93858	0.022	0.018
4	2.94825	0.000	0.041
5	2.95776	0.023	-0.000
6†	1.51506	0.087	0.119
7†	1.52717	0.032	0.290
8†	1.53426	1.316	-0.281

Table 9: Difference between the measured center-wavelength of CAA/REF lines in Cycle 1 and Cycle 2, for G395M. Lines where the difference is greater than 0.1 nm in at least one of the two slits are indicated by a dagger symbol.

Index	Line wavelength (C1) [μm]	Diff. A200_1 [nm]	Diff. A200_2 [nm]
0†	4.35813	0.117	0.037
1	4.37405	0.008	-0.001
2	4.39708	-0.099	0.024
3	4.40784	0.047	0.025
4†	4.42262	0.197	0.297
5†	4.43588	-10.784	0.813
6†	3.03005	0.249	0.148
7†	3.05428	-0.032	0.158
8†	3.06591	-1.172	-0.076

Table 10: Difference between the measured center-wavelength of CAA/LINE1 emission features in Cycle 1 and Cycle 2, using the two fixed-slit G140H spectra.

Index	Line wavelength (C1) [μm]	Diff. A200_1 [nm]	Diff. A200_2 [nm]
0	0.99339	0.023	-0.015
1	1.08341	0.031	-0.005
2	1.19407	0.036	0.012
3	1.33064	-	0.004
4	1.50087	0.008	0.026
5	1.71583	0.042	0.009

slits within the same cycle were derived as an estimate of our accuracy and found to be -0.005 ± 0.020 nm (over 10 lines), which has very similar RMS to that for the wavelength difference between cycles.

The difference between the center wavelength of the emission features of LINE2 in Cycle 1 and Cycle 2, from G235H spectra are listed in Table 11. Excluding again line 3 in A_200_1, the average and RMS of these differences over the 10 lines, in the two slits with absolute difference lower than 0.1 nm, are -0.010 ± 0.037 nm, compared to a difference between the lines in the two different slits within the same exposure of 0.010 ± 0.020 nm.

Finally, the difference between the lines CoGs of LINE3 in Cycle 1 and Cycle 2, from G395H spectra are listed in Table 12. The average and RMS of these differences over the 10 lines in the two slits with absolute difference lower than 0.1 nm are -0.010 ± 0.041 nm, compared to a difference between the lines in the two different slits within the same exposure of 0.015 ± 0.027 .

These results indicate that also the LINE sources are stable across the two test cycles within an accuracy level of 0.02 nm for LINE1 and 0.04 nm for LINE2 and LINE3.

3 SUMMARY AND CONCLUSIONS

Using the parametric models of NIRSpec optical properties for Cycle 1 and Cycle 2 of the FM2 CPV campaign, we were able to compare the line positions of four of the spectral reference sources of the CAA: the REF source and LINE1/2/3. Given our measurement uncertainties and relative calibration accuracy, we conclude that the CoGs of the REF absorption lines are stable within 0.01 nm across the two test cycles. The CoGs of the emission features of LINE1 are stable within 0.02 nm, while those of LINE2 and LINE3 are stable within 0.04 nm, across the two test cycles. We note that the temperature of the CAA during the two cycles was very similar, with value 39.3 K in Cycle 1 and 39.8 K in Cycle 2. The wavelength stability of the CAA sources over time and across thermal cycles is an important factor if one wants to use

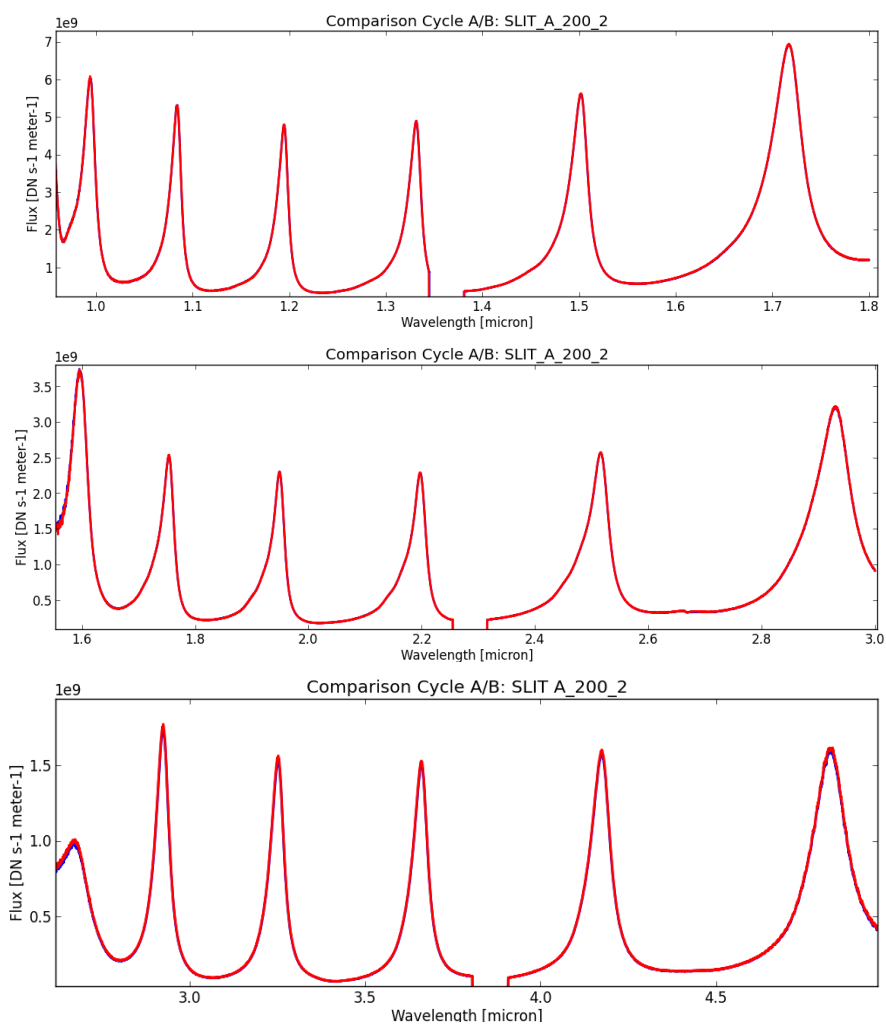


Figure 2: From top to bottom: G140H spectrum of CAA/LINE1, G235H spectrum of CAA/LINE2 and G395H spectrum of CAA/LINE3. All spectra are in grating order 1 and have been flat-fielded. The gap in the spectra is due to the gap between the two detector arrays in NIRSPEC focal plane. Cycle 1 data in blue and Cycle 2 data in red.

Table 11: Difference between the measured center-wavelength of CAA/LINE2 emission features in Cycle 1 and Cycle 2, using G235H spectra.

Index	Line wavelength (C1) [μm]	Diff. A200_1 [nm]	Diff. A200_2 [nm]
0†	1.59559	-0.097	-0.121
1	1.75258	-0.014	-0.024
2	1.94815	-0.008	0.031
3	2.19618	-	-0.015
4	2.51416	0.010	0.019
5	2.92779	-0.030	0.025

Table 12: Difference between the measured center-wavelength of CAA/LINE3 emission features in Cycle 1 and Cycle 2, using G395H spectra.

Index	Line wavelength (C1) [μm]	Diff. A200_1 [nm]	Diff. A200_2 [nm]
0	2.65905	0.658	-0.225
1	2.92303	-0.044	-0.033
2	3.25060	0.007	0.001
3	3.65857	-0.049	-0.048
4	4.17243	0.043	0.004
5	4.82520	0.065	-0.046

the CAA to monitor various instrument parameters, such as its geometrical distortions. The wavelength stability of these sources is also a fundamental requirements if we want to use them as reference in the optimization of the NIRSpec parametric model. For this purpose, an other crucial parameter is the number of lines for which the line center wavelength can be determined with sufficient accuracy for each gratings. It appears from this analysis, that the accuracy with which the center wavelength of nine REF absorption lines can be determined with the CoG method for all the high-resolution gratings is comparable to that achieved with a Gaussian fit for the narrow Argon emission lines (in the case of the fixed slits). The accuracy achieved for the medium-resolution gratings also appears to be sufficient (i.e. comparable to our model residuals) for an acceptable number of lines.

The accuracy with which the CoGs of the LINE emission features can be determined, for the H gratings, although slightly worse than that for the REF lines, would also be sufficient for the model optimization. Although in this case the number of lines is small, so one would use these in combination with the REF lines, anyway.

One parameter that is crucial to deriving reliable CoGs for these lines is the oversampling factor of the 1D-rectified spectrum, whose accuracy relies on the fixed slits spectral traces being approximately 30 pixels wide in spatial direction². For the parametric model optimization the MOS spectra have to be used as well and these have traces only 4 pixels wide, which will affect the accuracy of the over-sampling as well as the overall S/N of the spectra. However, the effect of this issue, as well as other aspects of using the internal lamps as opposed to the Argon source (such as wavelength coverage), are probably best assessed by performing the optimization itself and looking at how the residuals compares with those from the “Argon-optimized” model.

REFERENCES

- Alves de Oliveira, C. & Giardino, G. 2014, Algorithm to compute the unrectified 2D spectrum for NIRSpec fixed-slits, NIRSpec Technical Note NTN-2014-004, ESA
- Birkmann, S. 2011a, Description of the NIRSpec optical ground support equipment (OGSE), NIRSpec Technical Note NTN-2011-002, ESA/ESTEC
- Birkmann, S. 2011b, Description of the NIRSpec pre-processing pipeline, NIRSpec Technical Note NTN-2011-004, ESA/ESTEC
- Birkmann, S. 2013, NIRSpec wavelength calibration accuracy, NIRSpec Performance Report NPR-2013-007, ESA
- Boeker, T. & Giardino, G. 2011, Temporal Stability of CAA Lamp Fluxes, NIRSpec Performance Report NPR-2011-002, ESA
- Cameron, D. G., Kauppinen, J. K., Moffatt, D. J., et al. 1982, *Applied Spectroscopy*, 36, 245

²The Argon spectra used for the parametric model optimization were not over-sampled

- Dorner, B. 2012a, NIRSpec IPS Pipeline Software user manual, User Manual NIRS-MPI-MA-0002, MPI
- Dorner, B. 2012b, PhD thesis, Universite del Lyon
- Dorner, B. 2013, NIRSpec FM2 instrument model description, Note NIRS-MPI-TN-0013, MPI
- Giardino, G. 2013, An introduction to the NIRSpec parametric model, NIRSpec Technical Note NTN-2013-011, ESA/ESTEC